Journal of Theoretical Biology 540 (2022) 111090

Contents lists available at ScienceDirect

Journal of Theoretical Biology

journal homepage: www.elsevier.com/locate/yjtbi

Representing stimulus information in an energy metabolism pathway

Jay S. Coggan [a,*], Daniel Keller [a], Henry Markram [a], Felix Schürmann [a], Pierre J. Magistretti [b]

[a] Blue Brain Project, École Polytechnique Fédérale de Lausanne (EPFL), Geneva CH-1202, Switzerland
[b] Biological and Environmental Sciences and Engineering Division, King Abdullah University of Science and Technology (KAUST), Thuwal 23955, Saudi Arabia

ARTICLE INFO

Article history:
Received 6 April 2021
Revised 21 February 2022
Accepted 1 March 2022
Available online 7 March 2022

Keywords:
Ligand pulse
Dynamical systems
Cellular information
Biochemical networks
Metabolic states
Synthetic biology

ABSTRACT

We explored a computational model of astrocytic energy metabolism and demonstrated the theoretical plausibility that this type of pathway might be capable of coding information about stimuli in addition to its known functions in cellular energy and carbon budgets. Simulation results indicate that glycogenolytic glycolysis triggered by activation of adrenergic receptors can capture the intensity and duration features of a neuromodulator waveform and can respond in a dose-dependent manner, including non-linear state changes that are analogous to action potentials. We show how this metabolic pathway can translate information about external stimuli to production profiles of energy-carrying molecules such as lactate with a precision beyond simple signal transduction or non-linear amplification. The results suggest the operation of a metabolic state-machine from the spatially discontiguous yet interdependent metabolite elements. Such metabolic pathways might be well-positioned to code an additional level of salient information about a cell's environmental demands to impact its function. Our hypothesis has implications for the computational power and energy efficiency of the brain.

1. Introduction

The designs of brains reflect the challenges of processing and transmitting information in a way that is efficient in terms of information content and energy costs (Harris et al., 2015). This optimization has occurred at both the cellular and circuit levels as life has evolved from single cells to complex multicellular organisms, with more recent evolutionary processes built upon previous innovations. Even human intelligence, therefore, has deep roots in the computational history of rudimentary single-celled life (Dussutour et al., 2010; Schenz et al., 2019).

Although much work has already been done characterizing the considerable computational capabilities of single cells (e.g., Koch and Segev, 2000; Levin et al., 2011; Sterling and Laughlin, 2015), we believe that there could remain cellular features capable of processing information whose complexity and subtlety have thus far eluded full characterization. The focus of this paper is the prediction and theoretical exploration of a new way to represent information in a computational model of a metabolic energy pathway that could give single cells an expanded tool set for adaptation and decision making. This information coding would have been present from the dawn of cellular evolution since energy related pathways must have been present from the beginning and would have been a good substrate for beta-testing this kind of information processing techniques in enzymatic pathways.

The importance of information processing in single cells is widely acknowledged (Bhalla, 2014; Cardelli et al., 2017; Hernansaiz-Ballesteros et al., 2018; Jetka et al., 2019; Levin et al., 2011; Sterling and Laughlin, 2015). And even across species and deep into evolutionary history there are recurring themes of single-cell decision making (Balázsi et al., 2011; Boisseau et al., 2016). Because it is difficult to measure the spatiotemporal properties of biochemical fluxes, some theoretical guidance from computational models can be useful as they can be used as a tool to observe the behavior of new possible mechanisms in intracellular function (Ferrell et al., 2011).

The primary role of metabolism is the processing and regulation of a cell's energy and building supplies. The flux of matter through these pathways involves handing-off metabolite- products from one enzyme-catalyzed reaction to the next in the chain. Our results suggest that these pathways can also represent and transmit quantitative information about stimuli from neuromodulator binding to energy metabolite production and exhibit excitability states with concentration-dependent thresholds for non-linear response transitions (Coggan et al., 2020).

In this proof of concept, we make use of noradrenergic volume transmission onto an astrocyte that triggers a catabolic pathway involved in the recruitment of more energy production in the neuro-glia-vasculature (NGV) oligocellular unit to support

* Corresponding author.
E-mail address: jay.coggan@epfl.ch (J.S. Coggan).

https://doi.org/10.1016/j.jtbi.2022.111090
0022-5193/

increased activity in neighboring neurons through a process called the astrocyte-to-neuron lactate shuttle (ANLS) (Coggan et al., 2018a; Foote et al., 1983; Magistretti, 1994; Pellerin and Magistretti, 2012). This glycogenolysis-initiated glycolytic pathway captured the amplitude and duration of a range of input signals and delivered that information quantitatively to end product formation, with the option of responding to signals with non-linear state changes that are analogous to APs. The representation of both the intensity and duration of a stimulus, as well as the option of a non-linear response threshold, fulfil some of the basic requirements one would want if a metabolic pathway could quantitatively code information about the external environment. As we search for explanations for the energetic efficiency of the human brain, we suggest that the answer is likely to include expanded computational contributions from individual neurons.

2. Methods

The NGV computational model used in this report has been previously published and described (Coggan et al., 2020), the only difference here being the stimuli chosen. The glycogen module for this model was derived from (Xu et al., 2011), while the rest is based on (Jolivet et al., 2015) and also used in (Coggan et al., 2020, 2018b). Both the Matlab and NEURON code has now been open-sourced and can be found at this public repository: https://github.com/BlueBrain/Dynamical-State-Cell-Signaling-Simulator. In order to not repeat previously published schematics, the schematic overview in this paper focuses on pathway specifically examined, including the neuromodulator norepinephrine (NE) binding to its cognate beta-2 adrenergic receptor (β_2R), which triggers a cAMP-dependent mobilization of glucose from glycogen to feed into glycolysis and resulting in the production of the energy-carrying products lactate (LAC), ATP and NADH (Fig. 1**A**). Computationally, there are about 40 state variables involved and we refer the reader to the previous paper for additional schematic details beyond those provided in this paper (Coggan et al., 2020). We use glycolysis as the metabolic pathway test case because that is our laboratory's default subject of study. This pathway contains no cycles or allosteric features. The only branch point is at PYR, which can be converted to LAC or shuttled to the mitochondrion But the results and principles revealed by this model could be applied to any ligand-product chain-linked biomolecular network.

Three groups of NE waveforms were used as model stimuli in order to test the effects of 1) amplitude modulation, 2) time modulation and 3) both amplitude and time modulation combined. For each of these 3 categories of NE stimuli, 5 unique waveforms were generated from pairs of rise and decay time constants, τ_r and τ_d, respectively (Fig. 1**B**). The τ_r and τ_d values for all three groups of NE stimuli are listed in appendix 3, and the pairwise combinations can be assumed to be sequential.

The 5 concentrations of cAMP corresponding to stimulation states 1–5 for the ligand pulse (LP) analysis were obtained by setting $\times$ = 0.000009, 0.00002, 0.00005, 0.00008, or 0.00011 in equation 36 in appendix 1, where $\times$ is an arbitrary adenylate cyclase (AC) amplification factor covering the dose response span of the system (cf. (Coggan et al., 2020). Each colored plot (cyan, blue, green, red, and black) represents a different "state" of the metabolic cascade and came from an independent simulation with the correspondingly different concentration of cAMP generated by $\times$ (see Fig. 5). In this paper, downstream metabolite concentration trajectory shape changes observed for each cAMP-dependent level, as seen in plots of d[metabolite]/dt vs. [metabolite], are referred to as "state changes" and are similar to plots of dV/dt vs. V as traditionally used in neurophysiology to describe the non-linear dynamical features in phase plots of APs (e.g., Coggan et al., 2020; Yu et al., 2008). In the hysteresis curves for plots of [metabolite A] vs. [metabolite B], trajectory changes can also be observed at higher cAMP levels and these changes are also referred to as state changes that offer a view of the relative, mutual, non-linear dynamical variations of two different (usually but not necessarily tandem) metabolites in a cascade, in contrast to traditional derivative phase plots that only convey information about one metabolite. We posit that this novel way of looking at a metabolic pathway also communicates important information about the state of the cell's metabolic network and information processing bandwidth (Coggan et al., 2020). Although intractable for a single plot, the reader can imagine that all the metabolites in biochemical cascade or network varying in relation to each other would contain even more information.

All ligand-receptor dynamic simulations were performed in Matlab (R2016a, 64 bit) and the metabolic cascade was simulated in NEURON using a fixed time step of 3 μs with Euler integration. Matlab simulations were executed on an Intel i5 single-core laptop CPU running Ubuntu with 4 GB RAM, and the NEURON metabolic cascade simulations were conducted on an HPE supercomputer, the Blue Brain Project's BB5, hosted at the Swiss National Supercomputing Center (CSCS) in Lugano. Parameters and equations for the NEURON simulation environment model are listed in appendices 1 (Governing equations), 2 (Rates, transports and currents), and 3 (Parameters).

3. Results

3.1. Model and motivation

A computational model of neurmodulator-stimulated metabolic pathway transduction in an astrocyte, based on a previous study (Coggan et al., 2020, 2018b), was used to examine in finer detail the relationship between stimulus concentration waveforms (amplitude and duration characteristics), the affinity of the receptor, and the behavior of the metabolic pathway to the point of the production of a metabolite of interest.

For this case study, we used the neuromodulator norepinephrine (NE) as a stimulus ligand paired with the beta-2 adrenergic receptor (β_2R) to simulate neurotransmitter – receptor interactions. For the downstream metabolic pathway, we used the cAMP-dependent stimulation of glycogenolysis through glycolysis to the production of three energy transport molecules that form from pyruvate: lactate (LAC), ATP and NADH, with a particular interest in LAC which can be exported to the neighboring neuron in a process called ANLS (Pellerin and Magistretti, 2012). We focus on these aspects or products of the pathway to illustrate fundamental points involving the relationship between the waveform of a stimulating extracellular ligand and its cognate receptor affinity, and how information from this relationship can be transduced through metabolism to an end product (e.g., glycolysis and the production of energy carrying molecules) as a way of internally coding information about a cell's external environment, including demands for energy production.

$$NE \rightarrow \beta_2R \rightarrow cAMP \rightarrow \ldots PYR \rightarrow \{LAC, ATP, NADH\}$$

A schematic model of the metabolic pathway highlights the steps of interest (Fig. 1**A**), but this diagram only represents part of the larger model that includes neuron metabolism (details not shown) as previously described (Coggan et al., 2020, 2018b; Jolivet et al., 2015). These extra model capabilities do not affect this paper's focus. A range of NE waveforms were produced by modifying the rise and decay time constants (τ_r and τ_d, respectively, see Appendix A) in order to test the effects of amplitude, duration and combined amplitude and time variations (Fig. 1**B**).

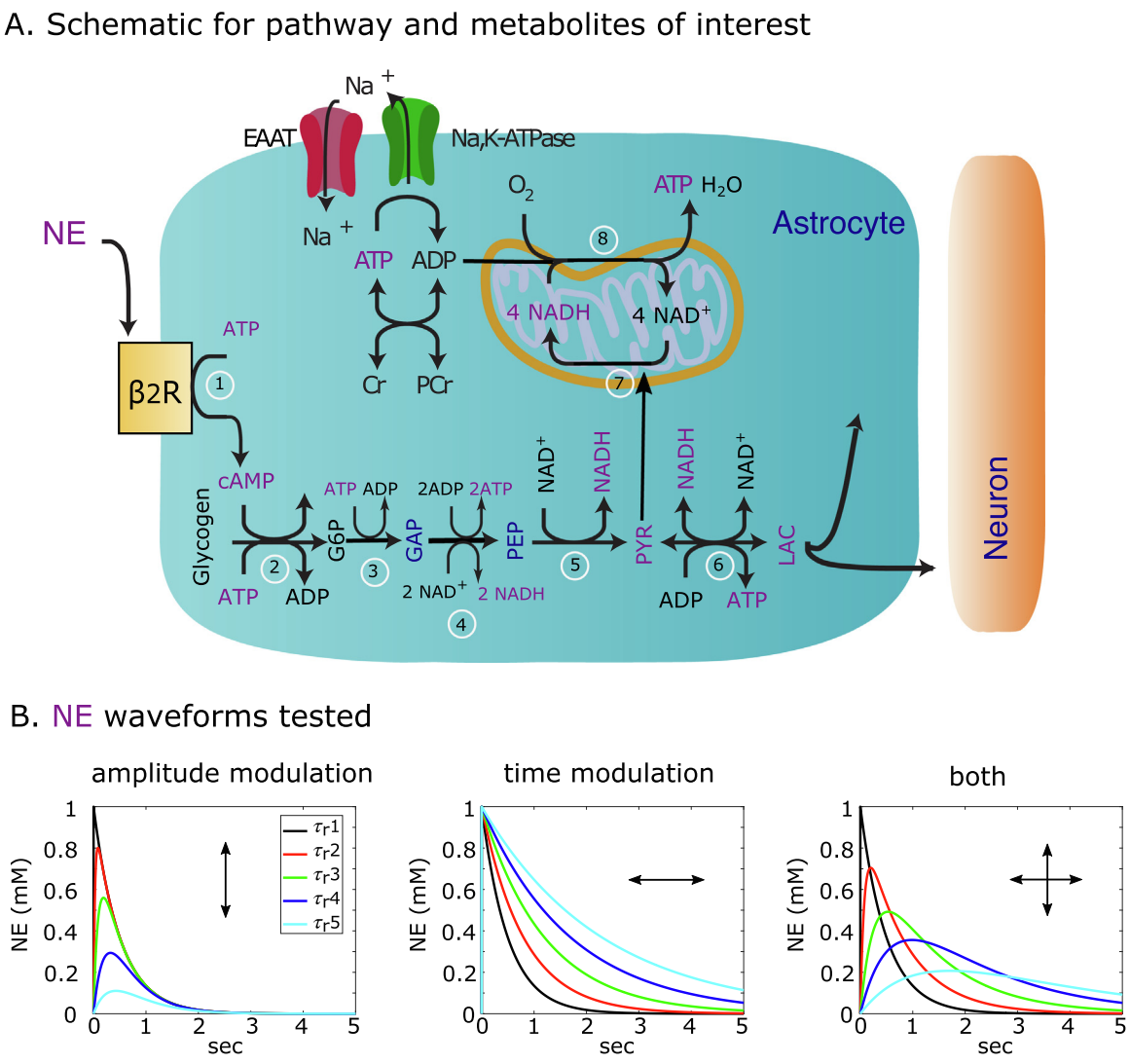

Fig. 1. Overview of key model elements, metabolites of interest and stimuli. A) Modeled metabolic pathway highlighting the neurotransmitter norepinephrine (NE) binding to the beta-adrenergic receptor (β_2R) on the surface of an astrocyte, triggering an AC amplification dependent, cAMP-triggered metabolic pathway involving the liberation of glucose from glycogen to enter glycolysis, the formation of its endpoint pyruvate (PYR) and downstream product alternatives lactate (LAC) in the cytosol, which can be exported to the extracellular space, or the energy currency molecules ATP and NADH derived from PYR transported to the mitochondrion. purple metabolites = emphasized metabolites in model results. Enumerated steps descriptions: 1) β_2R activation causes production of cAMP according to 5 different pre-programmed AC amplification factors (see methods for details), 2) chain of events from cAMP activating the catalytic subunits of protein kinase A (PKA), activation of protein phosphorylase 1 (PP1), activation of glycogen phosphorylase (GPa), production of glucose-6-phosphate (G6P) (see methods and appendices for details), 3) conversion rate for glyceraldehyde-3-phosphate (GAP) from 2 condensed enzymatic reactions, 4) condensed rate for phosphoenolpyruvate (PEP) from 3 sequential enzymatic reactions, 5) pyruvate kinase (PK) 6) lactate dehydrogenase (LDH), 7) transport of PYR to mitochondrion for oxidative metabolism to produce NADH (see methods and appendices for condensed formula) 8) production of ~32 ATP from ADP in mitochondrion (see methods and appendices) B) The neurotransmitter (NE) waveforms with amplitude (left panel), duration (middle panel) and combined amplitude and time variations (right panel). Direction-of-arrows symbols embedded in each panel will be used henceforth to indicate simulations involving modulation of amplitude, time or both.

3.2. Ligand-Receptor dynamics

The relationship between receptor affinities and neuromodulator waveforms. We probed the ability of a range of receptor K_ds (an inverse measure of affinity) to capture the amplitude and duration features of the neuromodulator waveform. Capture efficacies were assessed for all three categories of NE release shapes displayed in Fig. 1. Five ligand stimuli were generated from 5 different rise time constants (τ_r1 – black, τ_r2 - red, τ_r3 - green, τ_r4 - blue, τ_r5 – cyan; see **Appendix C** for values), which were applied to β_2Rs of 5 different K_ds (Fig. 2**A**; columns K_d5 through K_d1, highest to lowest, for exact values see **Appendix C**). The K_d-dependent time capture was assessed for each of the three waveform types (top row - vertical arrows signifying amplitude modulation, middle row - horizontal arrows signifying time modulation, and bottom row - crossed arrows signifying both amplitude and time modulation). The final column (K_d1, scaled) contains the same data as the penultimate column (K_d1), but is re-scaled to show how the waveform information is exactly captured by the lowest K_d receptor.

We then looked at K_d-dependent amplitude capture with the same procedure as for time, except here only the peaks of the responses are plotted in bar-graph form (Fig. 2B). The final column (K_d1, scaled) contains the same data as the penultimate column (K_d1), but is re-scaled to show how the amplitude information is exactly captured by the lowest K_d receptor. The results of these simulations and analysis suggest that low affinity receptors are always best for both amplitude and duration information capture and that high affinity receptors act as high-pass filters, which could be useful for coincidence detection. It was also observed that high affinity receptors spread the time responsiveness (see Fig. 2**A**,

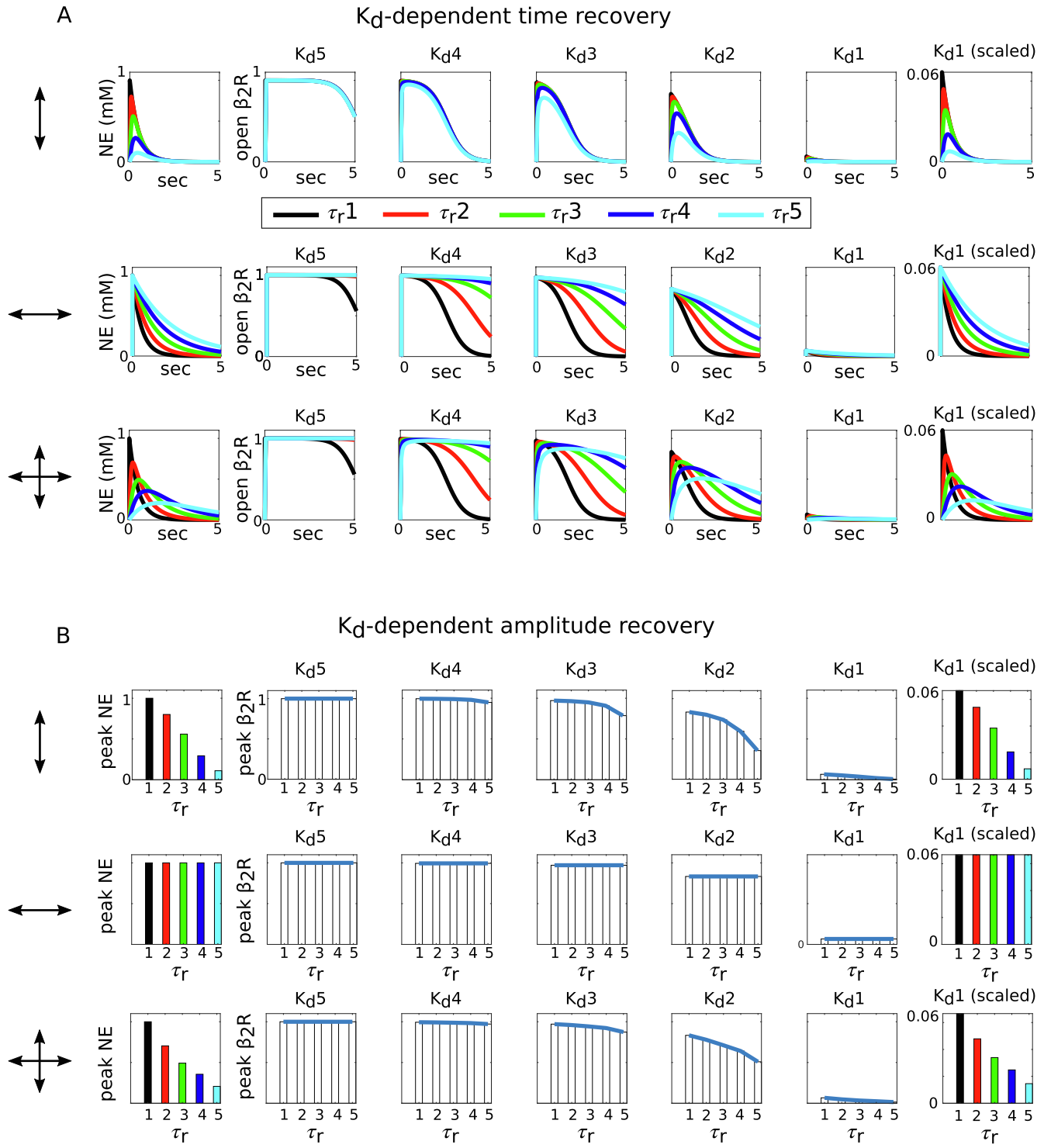

Fig. 2. Effects of receptor K_d on ligand waveform feature capture efficacy. A) K_d-dependent time recovery, for each of the three waveform types (top row - vertical arrows signifying amplitude modulation, middle row - horizontal arrows signifying time modulation, and bottom row - crossed arrows signifying both amplitude and time modulation), 5 ligand stimuli were generated from 5 different rise time constants (τ_r1 – black, τ_r2 - red, τ_r3 - green, τ_r4 - blue, τ_r5 - cyan), which were applied to β_2Rs of 5 different K_ds (columns K_d5 through K_d1, highest to lowest, for exact values see Methods). The final column (K_d1, scaled) contains the same data as the penultimate column (K_d1), but is re-scaled to show how the waveform information is exactly recovered by this low K_d receptor. B) K_d-dependent amplitude recovery. Same procedure as in (A) except here only the peaks of the responses are plotted in bar-graph form. The final column (K_d1, scaled) contains the same data as the penultimate column (K_d1), but is re-scaled to show how the amplitude information is exactly recovered by this low K_d receptor.

middle and lower rows). Another observation was that the amplitude capture for mixed responses Fig. 2**B** lower row, for example column K_d2, was different than for amplitude modulation alone (upper row, column K_d2).

We further explored the aforementioned "capture interference" observation: when time domain changes interfere with the capture of amplitude information. The peak β_2R amplitudes for each τ_r were plotted against each K_d for each of the 3 waveform groups,

A) amplitude modulation, B) time modulation, C) both (Fig. 3). In these plots we see that the range of amplitude responses for the mixed stimuli were less than that for amplitude only, suggesting that when time-domain variations were introduced to the stimuli, the ability of the receptor to faithfully capture amplitudes was compromised. This phenomenon was confirmed when we took the standard deviations for the range of response amplitudes for each group and plotted against the K_ds. While the standard deviations for the peak amplitudes of the time modulation responses were the lowest as expected, the standard deviations for the mixed group (diamond icon, dashed line) were not as large as for amplitude alone. This observation indicates that it is not possible to fully recover stimulus amplitude and duration simultaneously without a loss of information. In short, we predict the inability of a receptor to completely capture both the amplitude and duration characteristics of a stimulus, leading to some uncertainty about either or both measures of the signal (is there a ligand-receptor uncertainty principle?).

Ligand-receptor dynamics and receptor binding fraction. We created 6 ligand-receptor (L-R) pair types from 2 affinities (the lowest and the highest K_ds) and 3 waveforms that represented a broad range of τ_rs and τ_ds in order to examine the effects of neuromodulator dynamics and receptor affinity on β_2R binding fraction (Fig. 4**A**). Low affinity receptors produced very low receptor binding fractions, but provided an interesting result in so far as the τ_r of the stimulus was capable of increasing the binding fraction over the previous, slower τ_r, in one case as much as more than 60-fold (arrow in bar graph at L-R pair 3, Fig. 4**B**). This could be a significant regulatory point, even if in these extreme, proof-of-concept conditions the binding fractions at low affinity receptors were a fraction of those of high affinity receptors, where the τ_r was largely irrelevant. Thus, faster neurotransmitter dynamics can somewhat compensate for very low-affinity receptors to increase binding fraction, whereas high affinity receptors are oblivious to waveform dynamics due to saturation (L-R pairs 4,5 and 6, Fig. 4**B**).

3.3. Metabolic pathways can communicate L-R dynamics via linear responses or non-linear state-changes

Changes in the relative concentrations of ligands in an enzymatic cascade contain information about the stimulus amplitude and duration (Coggan et al., 2020; Tyson and Novak, 2001). These trajectories can be seen in the hysteresis plots of pairs of metabolites, tandem or otherwise. Supra-linear metabolite hysteresis curve changes are observed after a threshold has been passed. As in the preceding study, the cAMP-stimulated glycogenolytic glycolysis pathway was stimulated with 5 incremental AC amplification factors after NE- binding into 5 states (Fig. 5), represented in color codes black (cyclase factor 1), red (cyclase factor 2), green (cyclase factor 3), blue (cyclase factor 4) and cyan (cyclase factor 5). The precise amplification parameter values can be found in Appendix 3. The fastest and slowest neurotransmitter waveforms were coupled with the lowest and highest receptor affinities in order to investigate whether L-R dynamics can be expressed downstream in the responses of the glycolytic pathway, including ligand pulses (LPs) which are the representation of the non-linear state change observed in hysteresis plots that are similar to the transition from EPSPs to APs in embedding phase plots (Coggan et al., 2020). Pyruvate (PYR) was plotted against lactate (LAC, upper row), NADH (middle row) and ATP (lower row). For low affinity receptors (Fig. 5**A**) there is a clear difference in the LPs for fast and slow NE stimuli in the case of all three metabolic pairs, but for high-affinity receptors (Fig. 5**B**) there was no observable difference, suggesting that only low affinity receptors can be used to convey accurate intensity and time information about L-R dynamical properties through cascade states.

Phase plots (d[metabolite]/dt)/[metabolite]) of the derivatives of metabolite concentrations vs the self-same concentrations also reveal a non-linear state transition (LP) and these dynamics are reminiscent of the transition from excitatory postsynaptic potentials (EPSPs) to action potentials (APs). These non-linear dynamical embeddings suggest a new aspect of an intracellular language that expands previously narrow definitions of excitability and would increase the already formidable information processing capability of single cells from prokaryotes through higher metazoans.

Capturing stimulus duration with pathway states. After determining that LPs can reflect L-R dynamics for the speed of the stimulus, the next step was to assess whether information reflecting stimulus durations is similarly coded (Fig. 6). Once again, the slowest and fastest NE waveforms were coupled with the highest and lowest receptor affinities to form 4 test groups. An NE stimulation duration of × (in this case 20 msec) produces a transient cAMP response for each group along with an accompanying downstream PYR LP (essentially a PYR action potential) (Fig. 6**A**). We repeated this simulation with the same design as in (A) but with a 5x NE duration (now 100 msec) (Fig. 6**B**). For the low affinity receptors there is a clear state change in the LP between × and 5x stimuli (highlighted by dashed green boxes) but there was no difference for high-affinity receptors (highlighted by solid green boxes) suggesting that only low affinity receptors transmit information about stimulus duration to downstream metabolites.

3.4. Effector-site consequences of LRP dynamics

The next stage in the information transduction chain for a cell is the effect of the state dynamics on an output measure, or the effector at the end of the intracellular signalling; the

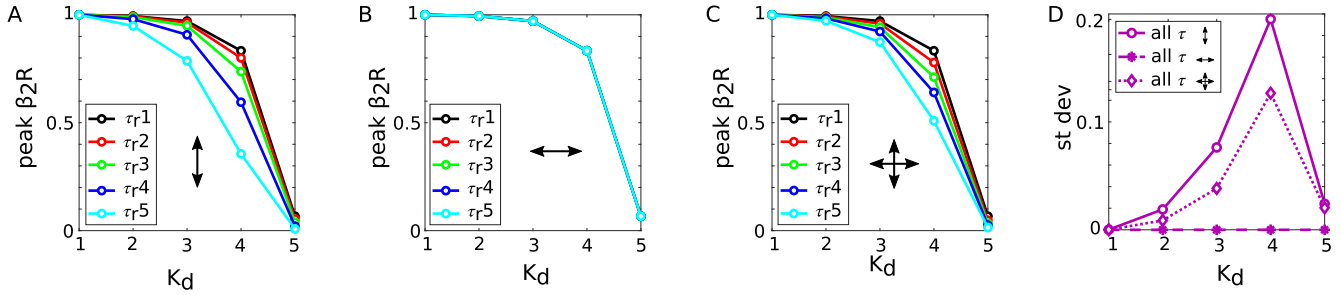

Fig. 3. Capture interference: when time domain changes interfere with the capture of amplitude information. The peak β_2R amplitudes for each τ_r were plotted against each K_d in each of the 3 waveform groups, A) amplitude modulation, B) time modulation, C) both. D) The standard deviations for the range of response amplitudes in for each group were plotted against the K_ds. While the standard deviations for the peak amplitudes of the time modulation responses were the lowest as expected, the standard deviations for the mixed group (diamond icon, dashed line) were not as large as for amplitude alone, indicating a loss of information transfer when an attempt is made to recover amplitude information and time information together.

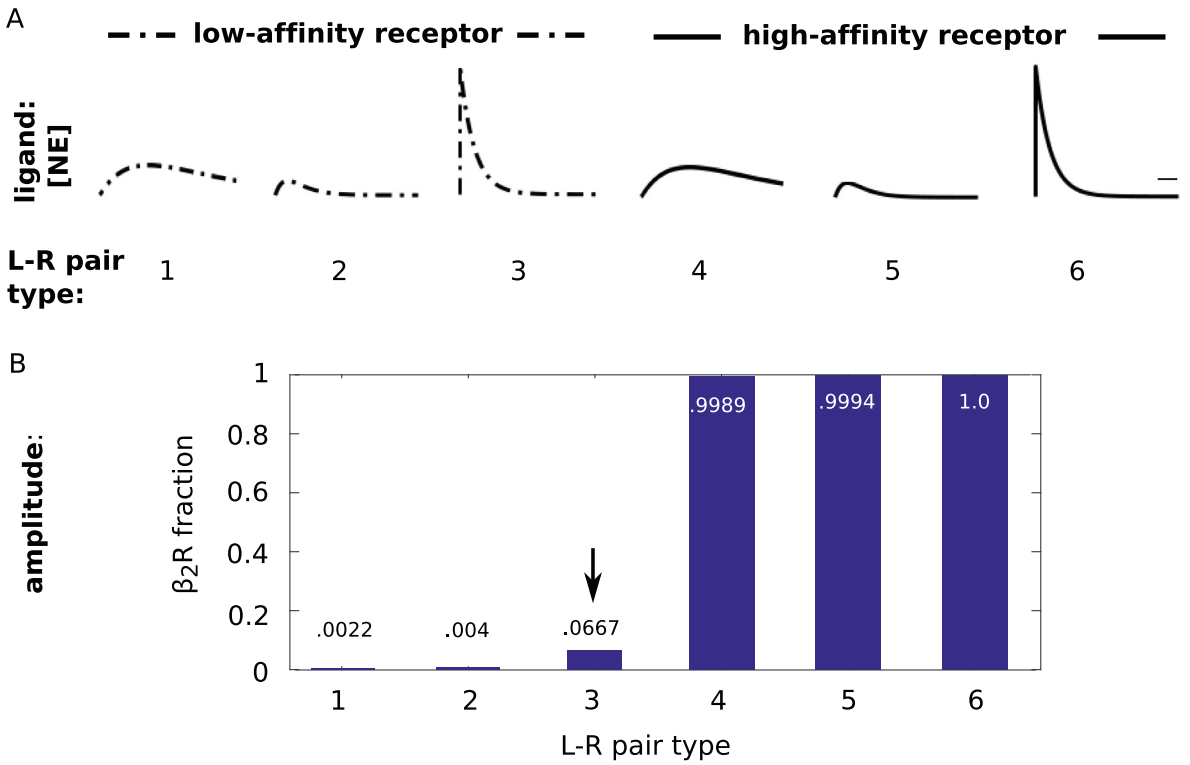

Fig. 4. Neurotransmitter dynamics and receptor affinity. A) Three diverse ligand waveforms (accounting for slow rise and slow decay, slow rise and fast decay, as well as fast rise and fast decay) together with two receptor affinities (K_ds) (the fastest and slowest in the study) were selected to examine the interaction of τ_r and K_d at the level of fractional β_2R binding, forming 6 ligand-receptor (L-R) pair types. B) Faster neurotransmitter dynamics can only slightly compensate for very low-affinity receptors to increase binding fraction. Arrow in bar graph points to response (L-R pair 3) where the fastest NE waveform can increase fractional binding at the low affinity receptor (compared to L-Rs 1 and 2), whereas the high affinity receptor is oblivious to waveform dynamics (L-R pairs 4,5 and 6).

dynamical messaging system acronym thus becoming LRPE (E for effector). As a case in point, we examined the downstream consequence of several LRP dynamical states at the level of LAC exportation from the astrocyte, a well-known component of the ANLS that has been described experimentally and computationally (Coggan et al., 2018b; Jolivet et al., 2015; Pellerin and Magistretti, 2012).

We simulated low and high affinity receptors (K_ds 14 and 3.6×10^{-5}, respectively) with fast NE stimuli at short (20 msec) and long (100 msec) durations for each of the 5 (AC) amplification factors, color-coded as in previous figures (Fig. 7). The LAC LP (dLAC/dt vs [LAC]) changes considerably with the change in duration at the low-affinity receptor (Fig. 7A, upper panels) as do the corresponding LAC export transients (Fig. 7A, vertically associated lower panels). The amplitude of the exported LAC reaches the response ceiling for the three highest cyclase amplification factors (green, red, black). At high-affinity receptors, there is only a subtle difference in the LAC LPs between short and long duration NE stimuli (observed at the lowest cyclase amplification, Fig. 7**B**, upper panels). This effect is reflected in the associated LAC exported amplitude change (Fig. 7**B**, lower panels). One also observes that after all transients corresponding to all cyclase amplifications reach the response ceiling amplitude, a secondary response characterized by a prolongation of the LAC export occurs (arrows in Fig. 7**B**, lower panels). This phenomenon conforms with the observations of the behaviour of response envelopes previously reported (Coggan et al., 2020), in that one dimension reaches a maximum before other or orthogonal dimensions can grow. Altogether, the differences in LAC transients as might be measured experimentally correspond to features in their associated LPs.

3.5. Ligand-Receptor-Pathway-Effector dynamics as a dose- and state-dependent system

The LRPE information transduction theory schematic diagram shows that cellular information is expressed in the coupled dynamics of the LRPE and that this constitutes the theoretical basis for a new kind of cellular information representing external stimuli that may have been overlooked due the difficulty in measuring it experimentally (Fig. 8). The corresponding specific case study components used in this study appear below the schematic diagram with: ligand is NE, receptor is β_2R at 5 different affinities ($K_d1 \rightarrow K_d5$), the metabolic pathway is cAMP- and state-dependent glycogenolytic glycogenolysis, and the effector was the production and export of the energy rich molecule lactate (LAC) for participation in the ANLS.

4. Discussion

The fields of biology and computing are mutually informative. Frequent measures of biological computing at both circuit and cellular levels include amplification, bistability, oscillations, covalent switches, state machines, feedback loops, intrinsic plasticity and other phenomena (Azeloglu and Iyengar, 2015; Bhalla, 2014; Goaillard and Marder, 2021; Koch and Segev, 2000; Miller, 2016; Tyson et al., 2008). But this extensive repertoire of tools is not likely complete. In single cells, from ligand-receptor binding to cell excitability, pathways stimulation, and the expression of gene products or other effector sites, there are many steps that provide opportunities for regulation and learning (Metallo and Vander Heiden, 2013). Many of these ideas are treated and studied in man-

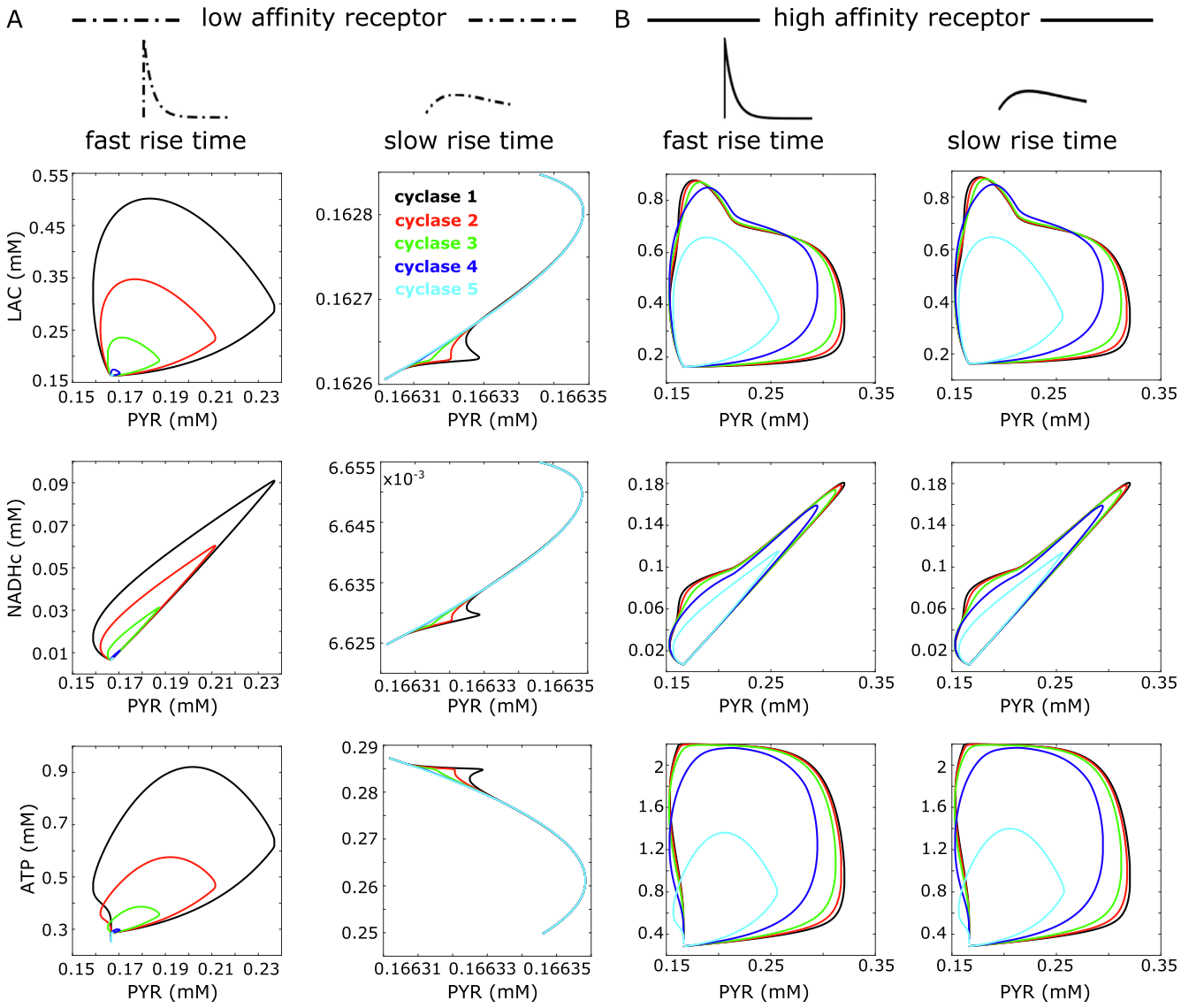

Fig. 5. Ligand-receptor pair types communicate information intracellularly through state-dependent LPs. The fastest and slowest neurotransmitter waveforms were coupled with the highest (solid lined NE) and lowest (dashed lined NE) receptor affinities in order to investigate whether L-R dynamics can be expressed downstream in LPs. PYR was plotted against LAC (upper row), NADH (middle row) ATP (lower row). For low affinity receptors (A, left columns) there is a clear difference in the LPs for fast and slow NE stimuli in the case of all three metabolic pairs, but for high-affinity receptors (B) there was no observable difference.

ageable experiments, but computational biology gives us the opportunity to explore new theoretical constructs (e.g., Beniaguev et al., 2021). What we show with our model is that metabolic pathways, which are primarily means of extracting energy and building block molecules from glucose and other substrates, might also be capable of coding detailed information about neuromodulators that stimulate increases in energy consumption.

4.1. Cellular computation implications

The hysteresis curves for tandem metabolite trajectories resemble the A vs B rotational dynamics plots (when B lags behind A in a time series) used in neuronal network analysis (Elsayed and Cunningham, 2017), suggesting metabolic pathways could operate similarly, but within a single cell. In these curves we observed the non-linear state change between the second and third stimulus level (Fig. 5, e.g, PYR vs. LAC), suggesting the ability of metabolic pathways to provide a kind of information similar to the transition between EPSPs and APs in neurons.

The mutual dependencies of the metabolites in a pathway, potentially provide a new dimension for communication in cells. Many metabolite concentrations are obligatorily connected for any given level of activation, this situation resembles the inner workings of an allosteric protein receptor except that the parts in the case of the biochemical pathway are discontiguous. In spite of their physical separation within the cell, they influence each other via concentration changes in a predictable way which seems to be similar to the state machine properties of receptors (Sterling and Laughlin, 2015). But within any metabolic network, enzymes and their products can be co-regulated by a number of mechanisms such as energy or substrate availability and anaplerotic portals, which together with the metabolite concentration-dependencies, significantly increase the number of possible system states metabolic pathways might assume, as well as their uncertainty, and therefore the number of bits they might store (Levin et al., 2011; Sterling and Laughlin, 2015). This dynamic would probably conform to well-known relationships between entropy and probability as formulated by Boltzmann with regard to molecular states and Shannon

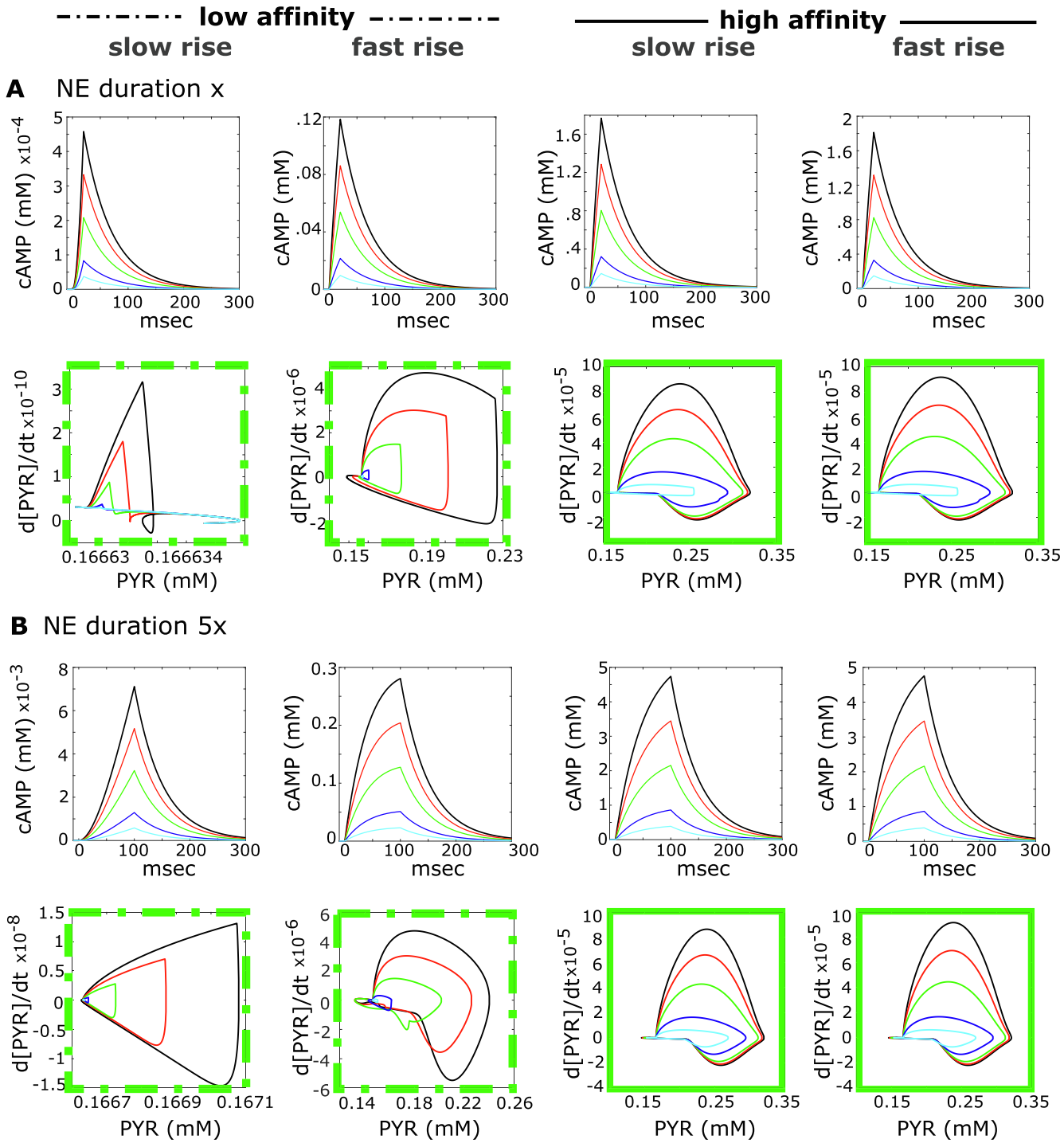

Fig. 6. Information reflecting stimulus durations is transmitted through cascade metabolite dynamics. The slowest and fastest NE waveforms are coupled with the highest (solid line) and lowest (dashed line) receptor affinities to form 4 test groups. A) An NE stimulation duration of × (in this case 20 msec) produces a transient cAMP response for each group along with an accompanying downstream pyruvate (PYR) LP. B) Same simulation design as in (A) but with a 5x NE duration (in this case 100 msec). For the low affinity receptors there is a clear state change in the LP between × and 5x stimuli but there is no difference for high-affinity receptors, suggesting that only low affinity receptors transmit information about stimulus duration to downstream metabolites.

(Shannon, 1948) with regard to information states, which equates the Gibbs entropy of a system with the number of bits needed to describe its constituent parts (Jaynes, 1965).

Fast information transmission is often accomplished with APs and evidence supports the existence of this capability in the LECA (Brunet and Arendt, 2016). While APs are considered faster than chemical diffusion, it is intriguing to consider whether the LP could fill an energy efficient information storage niche between a slower biochemical signal and evolution of a voltage-dependent AP (Liebeskind et al., 2011). A biochemical pathway already operating this way could respond rapidly and capture all the essential properties of stimuli changes beyond reaction–diffusion of metabolites (Bhalla, 2017; Bisegna et al., 2008). LPs are nearly identical to and APs based on their phase space embedding profiles (Coggan et al.,

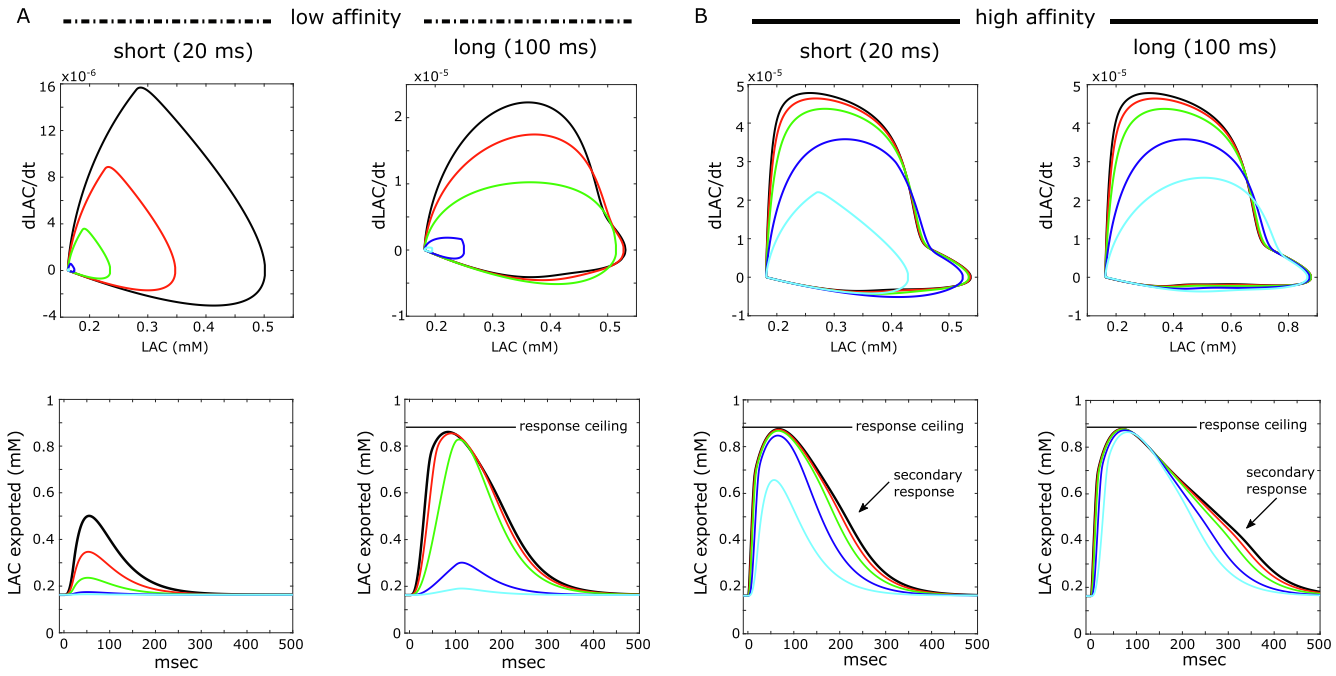

Fig. 7. Effector consequences of LRP dynamics. The downstream consequence of several LRP dynamical states at the level of LAC exportation from the astrocyte were examined. Low-affinity (**A**) and high-affinity (**B**) receptors (14 and 3.6 × 10^{-5}, respectively) were exposed to fast NE stimuli at short (20 msec) and long (100 msec) durations for each of the 5 AC amplification factors, color-coded as (cyclase 1 – black, cyclase 2 - red, cyclase 3 - green, cyclase 4 - blue, cyclase 5 - cyan). The LAC LP (dLAC/dt vs [LAC]) changes considerably with the change in duration at the low-affinity receptor (**A**, upper panels) as do the corresponding LAC export transients (vertically associated lower panels). The amplitude of the exported LAC reaches the response ceiling for the three highest cyclase amplification factors (green, red, black). At high-affinity receptors (**B**), there is only a subtle difference in the LAC LPs between short and long duration NE stimuli (observed at the lowest cyclase amplification, upper panels). This effect is reflected in the associated LAC exported amplitude change (lower panels). One also observes that after all transients corresponding to all cyclase amplifications reach the response ceiling amplitude, a secondary response characterized by a prolongation of the LAC export occurs (arrows in Fig. 7**B**, lower panels).

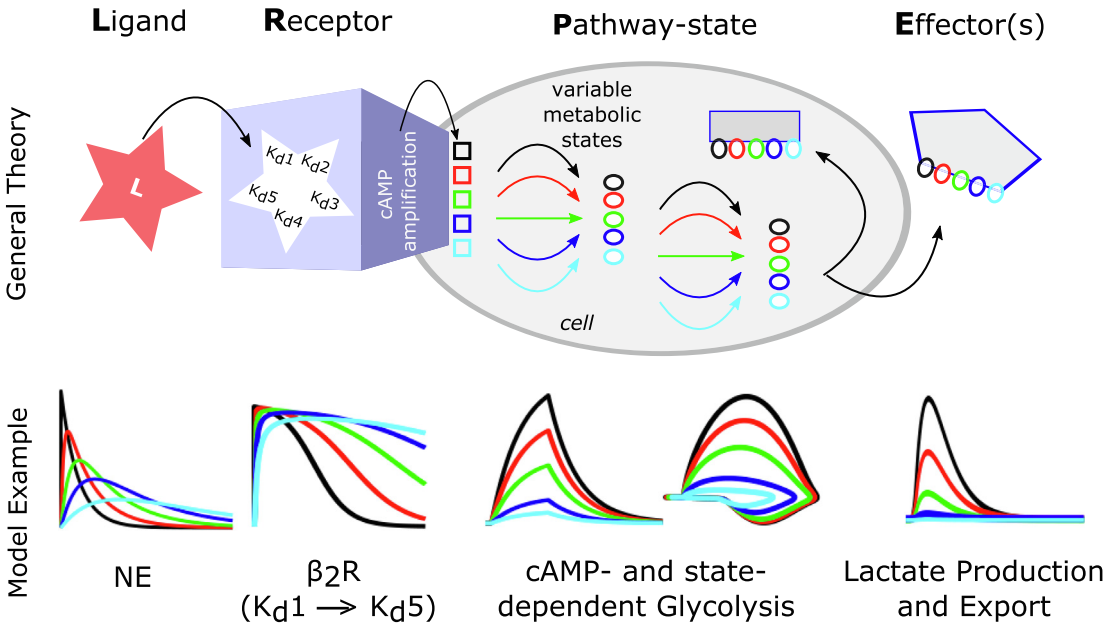

Fig. 8. Ligand-Receptor-Pathway(state)-Effector (LRPE) intracellular information processing theory. A) Schematic diagram shows that cellular information is contained the group dynamics of ligand, receptor, metabolic pathway state and effector site. B) the corresponding specific case study components used in this study: ligand is NE, receptor is β_2R at 5 different affinities ($K_d1 \rightarrow K_d5$), the metabolic pathway is cAMP- and state-dependent, and the effector was the production and export of the energy rich molecule LAC for participation in the ANLS.

2020; Takens, 1981; Yu et al., 2008). These features could be exploited to convey information about a stimulus engram-style in a metabolic pathway (Coggan et al., 2020; Pignatelli et al., 2019).

Receptor-affinity dependence. For low affinity receptors (Fig. 5**A**) there is a clear difference in the LPs for fast and slow NE stimuli in the case of all three metabolic pairs, but for high-affinity receptors there was no observable difference (Fig. 5**B**). There is lower dynamic range for LAC and NADH for slow τ_r at low affinity receptors since these responses are smaller due to a combination of the lack of responsiveness of the low affinity receptors and the forward

rates of their corresponding enzymes downstream from the initial stimulus. These results suggested that metabolic pathways can faithfully transduced information about L-R dynamics to the intracellular milieu only through low affinity receptors. High affinity receptors still communicate L-R information, but these effects are high-pass filtered. We propose that one of the reasons only low-affinity receptors can be used for high fidelity information transfer is that rise-times matter more than durations in terms of receptor activation (Fig. 4). This effect is similar to the observation that the fastest currents participating in voltage-dependent AP initiation and propagation are the most important for generating basic firing patterns in an axon (Coggan et al., 2010). Subcellular compartmentalization will very likely factor in the organization of information in any cell and will accordingly add another level of complexity (Bock et al., 2020; Jackson, 2020; Zhang et al., 2020).

4.2. Evolution implications

Much scientific inquiry explores the functions and evolution of single-celled organisms from prokaryotes to the more sophisticated eukaryotes (Wan and Jékely, 2021). In prokaryotes the spatial organization of the proteome is less defined than in eukaryotes. For example, oxidative metabolic reactions in prokaryotes may occur both in the cytosolic fluid and at the cell membrane, whereas they are largely confined to mitochondria in eukaryotes (Cloutier and Wellstead, 2010). Prokaryotes exhibit rudimentary stimulus-triggered AP-like activity that is less well-regulated than in eukaryotes, but similarly involved in information storage (Bruni et al., 2017; Yang et al., 2020). Whichever type of single-cell organism it is, it is clear they all possess considerable information processing powers. The metabolic pathway information transduction system we describe would have imbued these early life forms with even more enhanced computational capabilities. In this paper we have demonstrated that a metabolic pathway can code the amplitude and duration of a stimulus, while offering dose-dependent, non-linear state transitions (Figs. 6-8).

Although we use glucose metabolism to make these points, we do not see any reason why energy producing pathways should be treated any differently than other pathways. Given that the very earliest non-photosynthetic micro-organisms must have come equipped with chemical energy extracting mechanisms, it is not a stretch to imagine that strategies to process information about input signals using enzymatic cascades were worked-out with energy metabolism (Levin, 2006). For example, cyclic nucleotides play a central role in the transduction of external stimuli to various cellular consequences (Moya-Beltrán et al., 2019). Likewise, in our mammalian NGV system, a cyclic nucleotide mediates the request for more energy during brain activity as signaled by noradrenergic neuromodulation (Magistretti, 1994).

4.3. Synthetic biology

The principles uncovered by our computational approach might be applied to synthetic biology, a field on the cusp of changing biology (El Karoui et al., 2019). Much of the emphasis is on genetic, transcriptomic or proteomic manipulations to yield desired products (Casini et al., 2018; Collins, 2018). Synthetic biological circuits can be "programmed" at this level (Ausländer et al., 2012). But what determines output of a given input might very well include more intermediary processes before the nucleus knows what's happening, such as the signal amplitudes, concentration changes, biochemical switches, all of which might inform the "state" of a cell. These decision points may affect everything from the flow of energy, metabolic status or readout at the level of transcriptome products (Dusad et al., 2020). Even if it turns out that our LRPE pathway information theory is not used by evolved cells, it is possible that such molecular systems designs could find a place in synthetic biology.

5. Conclusion

Although much is already known about how single cells think or respond to their environment, they likely still have some undiscovered tricks. Our simulations of neuromodulator-stimulated glucose metabolism in an astrocyte suggest that metabolic pathways could be capable of more information processing than previously realized. These systems exhibit dose-dependent responses and states than can accurately capture the amplitude and duration properties of signals from L-R surface binding through metabolite fluxes and finally to a molecular product. They can also produce threshold-triggered state transitions with embedding features that resemble the transition from EPSPs to APs. Considering how many metabolic pathways are active simultaneously, these mechanisms could significantly increase the computational capabilities of neurons and help explain the efficient energy usage of brains.

Declaration of Competing Interest

The authors declare that they have no known competing financial interests or personal relationships that could have appeared to influence the work reported in this paper.

Acknowledgements

The authors thank the Molecular Systems group at the Blue Brain Project for helpful discussions and Alessandro Foni for the Graphical Abstract illustration. Supported by a CRG grant from King Abdullah University of Science and Technology "KAUST-EPFL Alliance for Integrative Modeling of Brain Energy Metabolism" [OSR-2017-CRG6-3438] (PJM); the Blue Brain Project, a research center of the École Polytechnique Fédérale de Lausanne, from the Swiss government's ETH Board of the Swiss Federal Institutes of Technology (HM); and NCCR Synapsy (PJM).

Appendix A. Supplementary data

Supplementary data to this article can be found online at https://doi.org/10.1016/j.jtbi.2022.111090.

References

Ausländer, S., Ausländer, D., Müller, M., Wieland, M., Fussenegger, M., 2012. Programmable single-cell mammalian biocomputers. Nature 487, 123–127. https://doi.org/10.1038/nature11149.

Azeloglu, E.U., Iyengar, R., 2015. Signaling networks: information flow, computation, and decision making. Cold Spring Harb. Perspect. Biol. 7,. https://doi.org/10.1101/cshperspect.a005934 a005934.

Balázsi, G., van Oudenaarden, A., Collins, J.J., 2011. Cellular decision making and biological noise: from microbes to mammals. Cell 144, 910–925. https://doi.org/10.1016/j.cell.2011.01.030.

Beniaguev, D., Segev, I., London, M., 2021. Single cortical neurons as deep artificial neural networks. Neuron 109, 2727–2739.e3. https://doi.org/10.1016/j.neuron.2021.07.002.

Bhalla, U.S., 2017. Synaptic input sequence discrimination on behavioral timescales mediated by reaction-diffusion chemistry in dendrites. Elife 6. https://doi.org/10.7554/eLife.25827.

Bhalla, U.S., 2014. Molecular computation in neurons: a modeling perspective. Curr. Opin. Neurobiol. 25, 31–37. https://doi.org/10.1016/j.conb.2013.11.006.

Bisegna, P., Caruso, G., Andreucci, D., Shen, L., Gurevich, V.V., Hamm, H.E., DiBenedetto, E., 2008. Diffusion of the second messengers in the cytoplasm acts as a variability suppressor of the single photon response in vertebrate phototransduction. Biophys. J. 94, 3363–3383. https://doi.org/10.1529/biophysj.107.114058.

Bock, A., Annibale, P., Konrad, C., Hannawacker, A., Anton, S.E., Maiellaro, I., Zabel, U., Sivaramakrishnan, S., Falcke, M., Lohse, M.J., 2020. Optical mapping of cAMP signaling at the nanometer scale. Cell 182, 1519–1530.e17. https://doi.org/10.1016/j.cell.2020.07.035.

Boisseau, R.P., Vogel, D., Dussutour, A., 2016. Habituation in non-neural organisms: evidence from slime moulds. Proc. Royal Soc. B: Biol. Sci. 283, 20160446. https://doi.org/10.1098/rspb.2016.0446.

Brunet, T., Arendt, D., 2016. From damage response to action potentials: early evolution of neural and contractile modules in stem eukaryotes. Philos. Trans. Royal Soc. B: Biol. Sci. 371, 20150043. https://doi.org/10.1098/rstb.2015.0043.

Bruni, G.N., Weekley, R.A., Dodd, B.J.T., Kralj, J.M., 2017. Voltage-gated calcium flux mediates *Escherichia coli* mechanosensation. Proc. Natl. Acad. Sci. 114, 9445–9450. https://doi.org/10.1073/pnas.1703084114.

Cardelli, L., Hernansaiz-Ballesteros, R.D., Dalchau, N., Csikász-Nagy, A., 2017. Efficient switches in biology and computer science. PLoS Comput. Biol. 13,. https://doi.org/10.1371/journal.pcbi.1005100 e1005100.

Casini, A., Chang, F.-Y., Eluere, R., King, A.M., Young, E.M., Dudley, Q.M., Karim, A., Pratt, K., Bristol, C., Forget, A., Ghodasara, A., Warden-Rothman, R., Gan, R., Cristofaro, A., Borujeni, A.E., Ryu, M.-H., Li, J., Kwon, Y.-C., Wang, H., Tatsis, E., Rodriguez-Lopez, C., O'Connor, S., Medema, M.H., Fischbach, M.A., Jewett, M.C., Voigt, C., Gordon, D.B., 2018. A pressure test to make 10 molecules in 90 days: external evaluation of methods to engineer biology. J. Am. Chem. Soc. 140, 4302–4316. https://doi.org/10.1021/jacs.7b13292.

Cloutier, M., Wellstead, P., 2010. The control systems structures of energy metabolism. J. R. Soc. Interface 7, 651–665. https://doi.org/10.1098/rsif.2009.0371.

Coggan, J.S., Calì, C., Keller, D., Agus, M., Boges, D., Abdellah, M., Kare, K., Lehväslaiho, H., Eilemann, S., Jolivet, R.B., Hadwiger, M., Markram, H., Schürmann, F., Magistretti, P.J., 2018a. A process for digitizing and simulating biologically realistic oligocellular networks demonstrated for the neuro-glio-vascular ensemble. Front. Neurosci. 12, 664. https://doi.org/10.3389/fnins.2018.00664.

Coggan, J.S., Keller, D., Calì, C., Lehväslaiho, H., Markram, H., Schürmann, F., Magistretti, P.J., 2018b. Norepinephrine stimulates glycogenolysis in astrocytes to fuel neurons with lactate. PLoS Comput. Biol. 14,. https://doi.org/10.1371/journal.pcbi.1006392 e1006392.

Coggan, J.S., Keller, D., Markram, H., Schürmann, F., Magistretti, P.J., 2020. Excitation states of metabolic networks predict dose-response fingerprinting and ligand pulse phase signalling. J. Theor. Biol. 487,. https://doi.org/10.1016/j.jtbi.2019.110123 110123.

Coggan, J.S., Prescott, S.A., Bartol, T.M., Sejnowski, T.J., 2010. Imbalance of ionic conductances contributes to diverse symptoms of demyelination. Proc. Natl. Acad. Sci. 107, 20602–20609. https://doi.org/10.1073/pnas.1013798107.

Collins, J.P., 2018. Gene drives in our future: challenges of and opportunities for using a self-sustaining technology in pest and vector management. BMC Proc. 12. https://doi.org/10.1186/s12919-018-0110-4.

Dusad, V., Thiel, D., Barahona, M., Keun, H.C., Oyarzún, D.A., 2020. Opportunities at the interface of network science and metabolic modelling. arXiv:2006.03286 [q-bio].

Dussutour, A., Latty, T., Beekman, M., Simpson, S.J., 2010. Amoeboid organism solves complex nutritional challenges. Proc. Natl. Acad. Sci. USA 107, 4607–4611. https://doi.org/10.1073/pnas.0912198107.

El Karoui, M., Hoyos-Flight, M., Fletcher, L., 2019. Future trends in synthetic biology—A report. Front. Bioeng. Biotechnol. 7. https://doi.org/10.3389/fbioe.2019.00175.

Elsayed, G.F., Cunningham, J.P., 2017. Structure in neural population recordings: an expected byproduct of simpler phenomena? Nat. Neurosci. 20, 1310–1318. https://doi.org/10.1038/nn.4617.

Ferrell, J.E., Tsai, T.-Y.-C., Yang, Q., 2011. Modeling the cell cycle: why do certain circuits oscillate? Cell 144, 874–885. https://doi.org/10.1016/j.cell.2011.03.006.

Foote, S.L., Bloom, F.E., Aston-Jones, G., 1983. Nucleus locus ceruleus: new evidence of anatomical and physiological specificity. Physiol. Rev. 63, 844–914. https://doi.org/10.1152/physrev.1983.63.3.844.

Goaillard, J.-M., Marder, E., 2021. Ion channel degeneracy, variability, and covariation in neuron and circuit resilience. Annu. Rev. Neurosci. 44, 335–357. https://doi.org/10.1146/annurev-neuro-092920-121538.

Harris, J.J., Jolivet, R., Engl, E., Attwell, D., 2015. Energy-efficient information transfer by visual pathway synapses. Curr. Biol. 25, 3151–3160. https://doi.org/10.1016/j.cub.2015.10.063.

Hernansaiz-Ballesteros, R.D., Cardelli, L., Csikász-Nagy, A., 2018. Single molecules can operate as primitive biological sensors, switches and oscillators. BMC Syst. Biol. 12. https://doi.org/10.1186/s12918-018-0596-4.

Jackson, P.K., 2020. cAMP signaling in nanodomains. Cell 182, 1379–1381. https://doi.org/10.1016/j.cell.2020.08.041.

Jaynes, E.T., 1965. Gibbs vs Boltzmann entropies. Am. J. Phys. 33, 391–398. https://doi.org/10.1119/1.1971557.

Jetka, T., Nienałtowski, K., Winarski, T., Błoński, S., Komorowski, M., 2019. Information-theoretic analysis of multivariate single-cell signaling responses. PLoS Comput. Biol. 15,. https://doi.org/10.1371/journal.pcbi.1007132 e1007132.

Jolivet, R., Coggan, J.S., Allaman, I., Magistretti, P.J., 2015. Multi-timescale modeling of activity-dependent metabolic coupling in the neuron-glia-vasculature ensemble. PLoS Comput. Biol. 11,. https://doi.org/10.1371/journal.pcbi.1004036 e1004036.

Koch, C., Segev, I., 2000. The role of single neurons in information processing. Nat. Neurosci. 3, 1171–1177. https://doi.org/10.1038/81444.

Levin, B.E., 2006. Metabolic sensing neurons and the control of energy homeostasis. Physiol. Behav. 89, 486–489.

Levin, R., Laughlin, S., De La Rocha, C., Blackwell, A.F. (Eds.), 2011. Energy, Information, and the Work of the Brain, in: Work Meets Life. The MIT Press. 10.7551/mitpress/7417.003.0005.

Liebeskind, B.J., Hillis, D.M., Zakon, H.H., 2011. Evolution of sodium channels predates the origin of nervous systems in animals. Proc. Natl. Acad. Sci. 108, 9154–9159. https://doi.org/10.1073/pnas.1106363108.

Magistretti, P.J., 1994. Vasoactive intestinal peptide and noradrenaline regulate energy metabolism in astrocytes: a physiological function in the control of local homeostasis within the CNS. Prog. Brain Res. 100, 87–93.

Metallo, C.M., Vander Heiden, M.G., 2013. Understanding metabolic regulation and its influence on cell physiology. Mol. Cell 49, 388–398. https://doi.org/10.1016/j.molcel.2013.01.018.

Miller, P., 2016. Dynamical systems, attractors, and neural circuits. F1000Research 5, 992. 10.12688/f1000research.7698.1.

Moya-Beltrán, A., Rojas-Villalobos, C., Díaz, M., Guiliani, N., Quatrini, R., Castro, M., 2019. Nucleotide second messenger-based signaling in extreme Acidophiles of the Acidithiobacillus species complex: partition between the core and variable gene complements. Front. Microbiol. 10, 381. https://doi.org/10.3389/fmicb.2019.00381.

Pellerin, L., Magistretti, P.J., 2012. Sweet sixteen for ANLS. J. Cereb.Blood Flow Metab 32, 1152–1166. https://doi.org/10.1038/jcbfm.2011.149.

Pignatelli, M., Ryan, T.J., Roy, D.S., Lovett, C., Smith, L.M., Muralidhar, S., Tonegawa, S., 2019. Engram cell excitability state determines the efficacy of memory retrieval. Neuron 101, 274–284.e5. https://doi.org/10.1016/j.neuron.2018.11.029.

Schenz, D., Nishigami, Y., Sato, K., Nakagaki, T., 2019. Uni-cellular integration of complex spatial information in slime moulds and ciliates. Curr. Opin. Genet. Dev. 57, 78–83. https://doi.org/10.1016/j.gde.2019.06.012.

Shannon, C.E., 1948. A mathematical theory of communication. Bell Syst. Tech. J. 27, 379–423. https://doi.org/10.1002/j.1538-7305.1948.tb01338.x.

Sterling, P., Laughlin, S., 2015. Principles of Neural Design. The MIT Press, Cambridge, Massachusetts.

Takens, F., 1981. Detecting strange attractors in turbulence, in: Rand, D., Young, L.-S. (Eds.), Dynamical Systems and Turbulence, Warwick 1980, Lecture Notes in Mathematics. Springer Berlin Heidelberg, Berlin, Heidelberg, pp. 366–381. 10.1007/BFb0091924.

Tyson, J.J., Albert, R., Goldbeter, A., Ruoff, P., Sible, J., 2008. Biological switches and clocks. J. R. Soc. Interface 5. https://doi.org/10.1098/rsif.2008.0179.focus.

Tyson, J.J., Novak, B., 2001. Regulation of the eukaryotic cell cycle: molecular antagonism, hysteresis, and irreversible transitions. J. Theor. Biol. 210, 249–263. https://doi.org/10.1006/jtbi.2001.2293.

Wan, K.Y., Jékely, G., 2021. Origins of eukaryotic excitability. Philos. Trans. R. Soc. B 376, 20190758. https://doi.org/10.1098/rstb.2019.0758.

Xu, K., Morgan, K.T., Todd Gehris, A., Elston, T.C., Gomez, S.M., 2011. A whole-body model for glycogen regulation reveals a critical role for substrate cycling in maintaining blood glucose homeostasis. PLoS Comput. Biol. 7,. https://doi.org/10.1371/journal.pcbi.1002272 e1002272.

Yang, C.-Y., Bialecka-Fornal, M., Weatherwax, C., Larkin, J.W., Prindle, A., Liu, J., Garcia-Ojalvo, J., Süel, G.M., 2020. Encoding membrane-potential-based memory within a microbial community. Cell Syst. 10, 417–423.e3. https://doi.org/10.1016/j.cels.2020.04.002.

Yu, Y., Shu, Y., McCormick, D.A., 2008. Cortical action potential backpropagation explains spike threshold variability and rapid-onset kinetics. J. Neurosci. 28, 7260–7272. https://doi.org/10.1523/JNEUROSCI.1613-08.2008.

Zhang, J.Z., Lu, T.-W., Stolerman, L.M., Tenner, B., Yang, J.R., Zhang, J.-F., Falcke, M., Rangamani, P., Taylor, S.S., Mehta, S., Zhang, J., 2020. Phase separation of a PKA regulatory subunit controls cAMP compartmentation and oncogenic signaling. Cell 182, 1531–1544.e15. https://doi.org/10.1016/j.cell.2020.07.043.